From Hygrophilic to Superhygrophobic: Theoretical Conditions for Making High-Contact-Angle Surfaces from Low-Contact-Angle Materials

Abraham Marmur†

Department of Chemical Engineering, Technion - Israel Institute of Technology, 32000 Haifa, Israel

Received January 29, 2008. Revised Manuscript Received April 15, 2008

The possibility of making high-contact-angle, rough surfaces from low-contact-angle materials has recently been suggested and demonstrated. A thermodynamic analysis of this possibility in terms of feasibility and stability is presented. It turns out that only roughness topographies that conform to a feasibility condition which is developed in the present paper can support this phenomenon. Even under conditions that support the phenomenon, the high-contact-angle state may not be stable, and transition from the heterogeneous (Cassie−Baxter) wetting regime to the homogeneous (Wenzel) regime with a lower contact angle may occur. In addition, it is suggested to use the general terms hygrophilic and hygrophobic (based on the Greek prefix *hygro-* that means liquid) to describe low- and high-contact-angle surfaces, respectively.

Introduction

Superhydrophobic (water-repellent) surfaces have attracted much attention during the past decade, due to their usefulness in many areas.[1−34] Superhydrophobicity is usually defined by a very high apparent contact angle (APCA), typically > ∼150°, and a very low roll-off angle (the inclination angle at which a water drop rolls off the surface), typically a few degrees. Since currently available materials have ideal (Young) contact angles with water that are lower than ∼120°, very high APCAs can be achieved only due to the effect of roughness.[35,36] It is well-known that wetting on rough surfaces can occur in either of two regimes:[27,35−37] (a) the homogeneous wetting regime, where the liquid completely penetrates into the roughness valleys, and (b) the heterogeneous wetting regime, where air is trapped inside the roughness valleys underneath the liquid. The term "air" will be used in this paper to indicate the gas with which the liquid and solid are in contact, which usually comprises air and vapor of the liquid.

For the most stable APCA[38] in the former regime, θ_W, the following equation was developed by Wenzel[35]

$$\cos\theta_W = r\cos\theta_Y \quad (1)$$

where r is the roughness ratio, defined as the ratio between the solid surface area and its projection, and θ_Y is the Young contact angle (CA) that applies to an ideal surface of the same chemistry. For the most stable APCA[38] in the heterogeneous wetting regime, θ_{CB}, the Cassie−Baxter (CB) equation[36] was developed:

$$\cos\theta_{CB} = r_f f\cos\theta_Y + f - 1 \quad (2)$$

In this equation, f is the fraction of the projected area of the solid surface under the drop that is wet by the liquid and r_f is the roughness ratio of the wet area. When $f = 1$, $r_f = r$, and the CB equation turns into the Wenzel equation. The validity of the Wenzel and CB equations, which has been recently questioned,[39] had been previously justified and explained,[40,41] as discussed below in the Theory section. A recent study[27] revealed a feasibility

† Fax: 972-4-829-3088. E-mail: marmur@technion.ac.il.

(1) Ahuja, A.; Taylor, J. A.; Lifton, V.; Sidorenko, A. A.; Salamon, T. R.; Lobaton, E. J.; Kolodner, P.; Krupenkin, T. N. *Langmuir* **2008**, *24*(1), 9–14.
(2) Tuteja, A.; Choi, W.; Ma, M.; Mabry, J. M.; Mazzella, S. A.; Rutledge, G. C.; McKinley, G. H.; Cohen, R. E. *Science* **2007**, *318*(5856), 1618–1622.
(3) Ma, Y.; Cao, X.; Feng, X.; Ma, Y.; Zou, H. *Polymer* **2007**, *48*, 7455–7460.
(4) Nosonovsky, M. *Langmuir* **2007**, *23*, 3157–3161.
(5) Zhang, J.; Gao, X.; Jiang, L. *Langmuir* **2007**, *23*(6), 3230–3235.
(6) Li, W.; Amirfazli, A. *Adv. Colloid Interface Sci.* **2007**, *132*(2), 51–68.
(7) Nosonovsky, M.; Bhushan, B. *Ultramicroscopy* **2007**, *107*(10−11), 969–79.
(8) Baldacchini, T.; Carey, J. E.; Zhou, M.; Mazur, E. *Langmuir* **2006**, *22*(11), 4917–4919.
(9) Pozzato, A.; Dal Zilio, S.; Fois, G. *Microelectron. Eng.* **2006**, *83*(4−9), 884–888.
(10) Ma, M.; Hill, R. M. *Curr. Opin. Colloid Interface Sci.* **2006**, *11*(4), 193–202.
(11) Gao, L.; McCarthy, T. J. *Langmuir* **2006**, *22*(7), 2966–2967.
(12) Yan, H.; Shiga, H.; Ito, E.; Nakagaki, T.; Takagi, S.; Ueda, T.; Tsujii, K. *Colloids Surf., A* **2006**, *284−285*, 490–494.
(13) Marmur, A. *Langmuir* **2006**, *22*(4), 1400–1402.
(14) Extrand, C. W. *Langmuir* **2006**, *22*(4), 1711–1714.
(15) Fuerstner, R.; Barthlott, W.; Neinhuis, C.; Walzel, P. *Langmuir* **2005**, *21*(3), 956–961.
(16) Callies, M.; Quere, D. *Soft Matter* **2005**, *1*(1), 55–61.
(17) Sun, T.; Feng, L.; Gao, X.; Jiang, L. *Acc. Chem. Res.* **2005**, *38*(8), 644–652.
(18) Jopp, J.; Gruell, H.; Yerushalmi-Rozen, R. *Langmuir* **2004**, *20*(23), 10015–10019.
(19) Marmur, A. *Langmuir* **2004**, *20*(9), 3517–3519.
(20) Patankar, N. A. *Langmuir* **2004**, *20*(19), 8209–8213.
(21) Otten, A.; Herminghaus, S. *Langmuir* **2004**, *20*(6), 2405–2408.
(22) Erbil, H. Y.; Demirel, A. L.; Avci, Y.; Mert, O. *Science* **2003**, *299*(5611), 1377–1380.
(23) Lau, K. K. S.; Bico, J.; Teo, K. B. K.; Chhowalla, M.; Amaratunga, G. A. J.; Milne, W. I.; McKinley, G. H.; Gleason, K. K. *Nano Lett.* **2003**, *3*(12), 1701–1705.
(24) Blossey, R. *Nat. Mater.* **2003**, *2*(5), 301–306.
(25) Bico, J.; Thiele, U.; Quere, D. *Colloids Surf., A* **2002**, *206*(1−3), 41–46.
(26) Nakajima, A.; Hashimoto, K.; Watanabe, T.; Takai, K.; Yamauchi, G.; Fujishima, A. *Langmuir* **2000**, *16*(17), 7044–7047.
(27) Marmur, A. *Langmuir* **2003**, *19*(20), 8343–8348.
(28) Neinhuis, C.; Barthlott, W. *Ann. Bot.* **1997**, *79*, 667–677.
(29) Saito, H.; Takai, K.-i.; Takazawa, H.; Yamauchi, G. *Mater. Sci. Res. Int.* **1997**, *3*(4), 216–219.
(30) Kako, T.; Nakajima, A.; Irie, H.; Kato, Z.; Uematsu, K.; Watanabe, T.; Hashimoto, K. *J. Mater. Sci.* **2004**, *39*(2), 547–555.
(31) Quere, D. *Rep. Prog. Phys.* **2005**, *68*, 2495–2532.
(32) Marmur, A. *Biofouling* **2006**, *22*(1/2), 107–115.
(33) Genzer, J.; Efimenko, K. *Biofouling* **2006**, *22*(5), 339–360.
(34) Callow, M. E.; Callow, J. A. *Biologist* **2002**, *49*(1), 10–4.
(35) Wenzel, R. N. *J. Ind. Eng. Chem.* **1936**, *28*, 988–94.
(36) Cassie, A. B. D.; Baxter, S. *Trans. Faraday Soc.* **1944**, *40*, 546–51.
(37) Johnson, R. E., Jr.; Dettre, R. H. *Contact Angle, Wettability, and Adhesion*; American Chemical Society: Washington, DC, 1964; pp 112−135.
(38) Marmur, A. *Soft Matter* **2006**, *2*, 12–17.
(39) Gao, L.; McCarthy, T. J. *Langmuir* **2007**, *23*, 3762–3765.
(40) Wolansky, G.; Marmur, A. *Colloids Surf., A* **1999**, *156*, 381–388.
(41) Brandon, S.; Haimovich, N.; Yeger, E.; Marmur, A. *J. Colloid Interface Sci.* **2003**, *263*, 237–243.

10.1021/la800304r CCC: $40.75
Published on Web 06/11/2008

condition that needs to be fulfilled in order for the heterogeneous wetting regime to exist:

$$d^2(r_f f)/df^2 > 0 \quad (3)$$

This condition shows that the heterogeneous (CB) regime may exist only for certain types of roughness topographies and that the transition between the two regimes does not depend only on the roughness ratio.

The Wenzel equation requires θ_Y to be higher than 90° in order to get the high APCAs needed for superhydrophobicity. The same is true for the CB equation when the surface roughness is made of "regularly" shaped ridges and valleys, as typically produced by random roughening processes (a detailed explanation will be given below). Such Young CAs are usually achievable with water; however, there is obviously much interest in liquid repellency in general. Therefore, the question of getting surfaces with high APCAs (≫90°) from materials with low CAs (<90°) has been raised. This does not seem to be feasible in the homogeneous wetting regime, since the Wenzel equation does not account for such a possibility. However, the CB equation does allow it, in principle, in the heterogeneous wetting regime. Two methods have been suggested to achieve this goal, the first of which utilizes closed-pore surfaces.[42] The mechanism of this method is quite obvious: liquid penetration into the closed pores causes an increase in pressure, which, in turn, prevents further penetration; this constraint imposes the heterogeneous wetting regime and leads to high APCAs.

The second method makes use of rough surfaces with multivalued topography (other terms used to describe such surfaces were re-entrant, self-affine, and specific terms such as mushroom-type or micro-hoodoos).[1–3,8,42,43] The term "multivalued topography" implies that a line drawn vertically up from a given point on the projection of the solid surface may meet the actual solid interface more than once, such as, for example, in the case of a surface made of mushroom-shaped bulges (see Figure 1a). In this case (in contrast to the first method), the roughness valleys are interconnected and also connected to the outside atmosphere; therefore, liquid and air can exchange positions without constraints, depending only on thermodynamic preferences. This method has been experimentally demonstrated;[1–3,8] however, the theoretical explanation has not been complete. The objective of the present paper is to theoretically study the conditions under which a low-CA material may be transformed into a high-APCA surface by using multivalued roughness topography. For this purpose, it is necessary to generalize the CB equation as well as the feasibility condition.

It is also suggested to use the terms hygrophilic and hygrophobic (from the Greek prefix *hygro-* that means liquid) to describe in general low-CA and high-CA surfaces. These terms can prevent the need for using multiple adjectives such as hydrophilic/oleophilic or hydrophobic/oleophobic.

Theory

The theory described in this paper generalizes the previous analysis of wetting regimes on rough surfaces[27] to include the case of multivalued roughness topography. Three examples of such topographies are shown in Figure 1a. The top one represents a "pure" convex shape of roughness features; the middle one represents a "pure" concave shape; and the bottom one shows a mushroom-type surface which is convex at its upper part and concave at its lower part. As will be shown below, there is a major difference between such surfaces in terms of the thermodynamically feasible wetting regime. The need for generalization of the previous theory stems from the fact that for multiple-valued topographies the solid−liquid area is not a unique function of the liquid−air area. This is demonstrated by the very simplified example given in Figure 1b and c, where there are two different values of solid−liquid area for the same value of the liquid−air area. Such a possibility is in contrast to the implicit assumption underlying the CB equation, namely that, for each area fraction of the liquid−air interface, $(1 - f)$ in eq 2, there is a single value of the projected area fraction of the solid−liquid interface, given by f. The considerations related to multivalued topographies do not affect the Wenzel equation, because the roughness ratio can be defined in the same way as for single-valued topographies. In addition, as mentioned above, the Wenzel equation does not allow the possibility of surfaces of high APCAs to be made of materials of low Young CAs. Therefore, the following discussion is focused on the generalization of the CB equation and the feasibility condition.

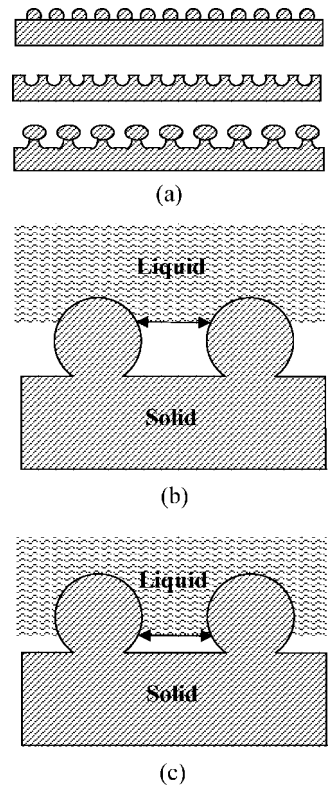

Figure 1. (a) Examples of multivalued roughness features: (top) convex features, (middle) concave features, and (bottom) mixed convex and concave features. Panels (b) and (c) show two states of the liquid−air interface that have the same liquid−air area and different solid−liquid area.

As is well-known, the equilibrium APCA is calculated by minimizing the Gibbs energy of the system. It is convenient (though not necessary[27]) to perform the minimization under the constraint of a constant volume of the liquid drop. In general, the Gibbs energy for rough or chemically heterogeneous surfaces displays multiple minima, and there is no universal way to identify the global minimum (most stable APCA). The useful approach taken by Wenzel, Cassie, and Baxter was to define a seemingly uniform surface with average properties that represent the physical or chemical heterogeneity.[35,36] The Gibbs energy on this seemingly uniform surface has a single minimum that can be easily defined, as in the case of a truly ideal surface. It was rigorously proven for rough surfaces[40] and numerically dem-

(42) Liu, J.-L.; Fenf, X.-Q.; Wang, G.; Yu, S.-W. *J. Phys.: Condens. Matter* **2007**, *19*, 356002.
(43) Herminghaus, S. *Europhys. Lett.* **2000**, *52*(2), 165–170.

onstrated for heterogeneous surfaces[41] that the averaging concept of Wenzel, Cassie, and Baxter is fully justified when the drop is sufficiently large compared with the scale of heterogeneity. It is important to emphasize that the averaging concept cannot be expected to hold when the drop is not sufficiently large. Therefore, this concept will be applied also in the present analysis, assuming that the ratio of drop size to roughness scale is sufficiently large. Numerical demonstrations[41] seem to suggest that a ratio of 2−3 orders of magnitude is sufficient; such a ratio is easily achieved in practice.

In general, the Gibbs energy of a solid−liquid−air system is given by

$$G = \sigma_l A_l + \sigma_{sl} A_{sl} + \sigma_s A_s \tag{4}$$

where σ is a surface/interfacial tension, A is an interfacial area, and the subscripts s and l stand for the solid and liquid, respectively. For simplicity, it is assumed that the effect of gravity is negligible (as is well-known, gravity affects the shape of the drop but not its CA). Under this condition, the pressure inside the liquid drop must be uniform. The air pressure is also uniform and equal to the atmospheric pressure, since the roughness valleys are interconnected among themselves and connected to the outside atmosphere. Therefore, the curvature must be the same for all liquid−air interfaces; that is, the curvature of the liquid−air interfaces inside the roughness valleys must equal that of the outside surface of the drop. Since the fundamental assumption underlying the concept of averaging the properties of the solid surface is that the drop radius is much larger than the roughness scale, the curvature of the liquid−air interfaces inside the roughness valleys is much lower than that of the roughness features. In addition, these interfaces have to adjust their shape in such a way that the actual contact angle with each solid surface of the roughness features will be the ideal contact angle.[44] This condition can be fulfilled in accord with the previous one by having positive and negative radii of curvature that still make the mean curvature very low. However, such a situation is not amenable to analytical formulation and requires difficult numerical calculations for each specific case. Therefore, as a first order approximation, the low curvature of these interfaces is assumed to imply that they are planar.

Also, because of the assumption that the drop is large compared with the scale of roughness, the volume of liquid inside the roughness valleys is negligible compared with the drop volume. This can be demonstrated by a simple order of magnitude analysis. The volume of the liquid in the roughness valleys can be estimated by $\pi R_b^2 h/2$, where R_b is the radius of the base of the drop, h is a typical depth of the roughness valleys, and the porosity of the roughness layer is assumed, for simplicity, to be 50%. The volume of the drop is conservatively estimated, by assuming a contact angle of 90°, to be $2\pi R_b^3/3$. The ratio of these volumes is $\sim h/R_b$. With typical orders of magnitude of $h \sim O[1\ \mu m]$ and $R_b \sim O[1$ mm], the volume of the liquid in the roughness valleys is indeed negligible. Similarly, the projected area of the perturbations in the contact line is negligible compared with the base area of the drop. In addition, line tension effects are assumed negligible.[45]

The interfacial areas and drop radius can be calculated as follows. The liquid−air interfacial area consists of two parts, the outside interface of the drop (a spherical cap) and the liquid−air interface within the roughness valleys:

$$A_l = 2\pi R^2(1 - \cos\theta) + f_l \pi R^2 \sin^2\theta \tag{5}$$

Here, R is the radius of the spherical drop, θ is the geometric APCA (the term geometric implies that this is not necessarily an equilibrium APCA), and f_l is the fraction of the base area of the drop which is exposed to the air inside the roughness valleys ($0 \le f_l \le 1$ corresponds to $(1 - f)$ in eq 2). The solid−liquid interfacial area is given by

$$A_{sl} = \pi R^2 f_{sl} \sin^2\theta \tag{6}$$

where f_{sl} is the wetted solid area per unit base area of the drop (f_{sl} may be greater than 1, and it corresponds to $r_f f$ in eq 2). The main point in the present analysis is that, unlike in the theory underlying eq 2, f_{sl} is not a single-valued function of f_l.

The solid-air interfacial area is simply expressed as the difference between the total solid surface area (which is constant), A_{total}, and the wetted solid area:

$$A_s = A_{total} - A_{sl} = A_{total} - \pi R^2 f_{sl} \sin^2\theta \tag{7}$$

The drop radius is related to its volume by

$$R^2 = \left(\frac{3V}{\pi}\right)^{2/3} (2 - 3\cos\theta + \cos^3\theta)^{-2/3} \tag{8}$$

Introducing eqs 5–8 into eq 4, the expression for the Gibbs energy can be written in the following dimensionless form

$$G^* \equiv \frac{G}{\sigma_l \pi^{1/3} (3V)^{2/3}} = F^{-2/3}(\theta)(2 - 2\cos\theta - \Omega \sin^2\theta) \tag{9}$$

where

$$F(\theta) \equiv (2 - 3\cos\theta + \cos^3\theta) \tag{10}$$

and

$$\Omega \equiv f_{sl} \cos\theta_Y - f_l \tag{11}$$

It should be noted that A_{total} is a constant that does not affect the minimization; therefore, it is taken as zero, for convenience. For single-valued roughness topographies, f_{sl} is a single-valued function of f_l. Therefore, the CB equation and the feasibility condition could be developed by considering G^* to be a function of two independent variables: θ and f_l (that corresponds to $(1 - f)$ in eq 2).[27] In the present case, instead of f_l, a different independent variable is required, of which f_{sl} and f_l are single-valued functions. To this end, it is convenient to use z, the depth of liquid penetration beneath the top of the roughness peaks, and have $f_{sl} = f_{sl}(z)$ and $f_l = f_l(z)$.

The necessary conditions for local extrema consist of vanishing of the first partial derivatives (assuming the function is differentiable). Applying these conditions to G^* one gets

$$\frac{\partial G^*}{\partial z} = -F^{-2/3}(\theta) \sin^2\theta \left(\cos\theta_Y \frac{df_{sl}}{dz} - \frac{df_l}{dz}\right) = 0 \tag{12}$$

$$\frac{\partial G^*}{\partial \theta} = 2F^{-5/3} \sin\theta(\Omega - \cos\theta)(1 - \cos\theta)^2 = 0 \tag{13}$$

Since $(4 > F > 0)$ for $\theta > 0$, eq 13 is fulfilled (for $\theta > 0$) when

$$\cos\theta \equiv \cos\theta_{CB} = \Omega = f_{sl} \cos\theta_Y - f_l \tag{14a}$$

This generalized equation has the same form as the CB equation; therefore, in order to avoid confusion, it is suggested to continue using the term "CB equation". For single-valued roughness topographies, this equation is indeed identical to the CB equation; the generalization covers the case for which f_{sl} is not related to f_l in a unique way. Equation 13 is also fulfilled when

(44) Wolansky, G.; Marmur, A. *Langmuir* **1998**, *14*, 5292–5297.
(45) Marmur, A.; Krasovitski, B. *Langmuir* **2002**, *18*, 8919–8923.

$$\theta=\pi \tag{14b}$$

Equation 12 is fulfilled when

$$\frac{df_{sl}/dz}{df_l/dz}=(\cos\theta_Y)^{-1} \tag{15a}$$

This equation is equivalent to the statement that the actual contact angle, which the liquid makes with the solid inside the roughness valleys, must be the Young contact angle,[27] as will be later demonstrated. Equation 12 is also fulfilled when

$$\theta=\pi \tag{15b}$$

Similarly to the conclusion in the previous analysis,[27] the only two meaningful combinations of the above four equations are as follows: (a) the contact angle being determined by eq 14a, with z being determined by eq 15a, and (b) $\theta=\pi$ and $z=0$. If both situations are possible and different from each other, the former turns out to be the more stable one, since it is associated with a lower contact angle.

As previously realized,[27] in addition to eqs 14a and 15a, the following condition must be met for a local extremum to exist:

$$AC-B^2>0 \tag{16}$$

where (assuming that the first derivatives are differentiable)

$$A\equiv\frac{\partial^2 G^*}{\partial z^2}=-F^{-2/3}\sin^2\theta\left(\cos\theta_Y\frac{d^2f_{sl}}{dz^2}-\frac{d^2f_l}{dz^2}\right) \tag{17}$$

$$B\equiv\frac{\partial^2 G^*}{\partial\theta\ \partial z}=2F^{-5/3}\sin\theta(1-\cos\theta)^2\left(\cos\theta_Y\frac{df_{sl}}{dz}-\frac{df_l}{dz}\right) \tag{18}$$

and

$$C\equiv\frac{\partial^2 G^*}{\partial\theta^2}=2F^{-5/3}(\Omega-\cos\theta)[\cos\theta(1-\cos\theta)^2+2\sin^2\theta(1-\cos\theta)-5F^{-1}\sin^4\theta(1-\cos\theta)^2]+2F^{-5/3}\sin^2\theta(1-\cos\theta)^2 \tag{19}$$

When $AC-B^2=0$, there may be, but does not need to be, a local extremum, and the function needs to be further checked in order to verify it. If eq 16 is not fulfilled, the Gibbs energy has a saddle point (see an example in Figure 4a, which is discussed in detail below) and the minimum is found at the border value of $f_l=0$, namely, at the Wenzel (homogeneous wetting) regime.

At the f_{sl} and f_l values that are necessary for a local minimum, $B=0$, by eqs 18 and 15a. Therefore, the existence of local extrema is determined only by the value of AC. For θ given by eq 14a

$$AC=-2F^{-7/3}\sin^4\theta(1-\cos\theta)^2\left(\cos\theta_Y\frac{d^2f_{sl}}{dz^2}-\frac{d^2f_l}{dz^2}\right) \tag{20}$$

Since F is always positive for $\theta>0$, a local extremum in G^* exists only if

$$\frac{d^2f_l}{dz^2}-\cos\theta_Y\frac{d^2f_{sl}}{dz^2}>0 \tag{21}$$

This is the generalized feasibility condition, which is markedly different from the one developed for the single-valued topography, eq 3. The nature of the extremum is determined by the sign of A: it is a minimum when $A>0$.[27] According to eqs 17 and 20, the sign of A is the same as the sign of AC. Thus, if the feasibility condition is fulfilled, the extremum must be a minimum.

Results and Discussion

The Gibbs energy of a drop on a rough surface depends on two independent variables: the extent of penetration into the roughness valleys and the geometric APCA of the drop. These two variables must be considered simultaneously when determining the minimum in the Gibbs energy, that is, the equilibrium state. An analysis of the local CA inside the roughness valleys, for example, without simultaneously considering the APCA of the whole drop may be misleading. Moreover, as shown in this paper and its precedent,[27] it is insufficient to consider only the equilibrium conditions for both the APCA, eq 14a, and the local CA inside the roughness valleys, eq 15a. The analysis must also show that the energy does not have a saddle point (as in Figure 4a) when the two first derivatives equal zero (eqs 14a and 15a). This is the meaning of the feasibility condition.

For single-valued roughness topographies, the left-hand side of eq 15a is always negative. This is so, because for such topographies f_l (the fraction of the base area of the drop that is exposed to the air inside the roughness valleys) decreases when the liquid penetrates more deeply into the roughness, whereas f_{sl} (the wetted solid area per unit base area of the drop) always increases. Therefore, equilibrium in the heterogeneous wetting regime for single-valued roughness topographies can be attained only for hygrophobic materials ($\cos\theta_Y<0$). The main questions asked in this paper are as follows: (a) Can the heterogeneous wetting regime exist for low Young contact angles (<90°) due to the multivalued nature of the roughness topography? (b) Can high APCAs as needed for superhygrophobicity be achieved in these heterogeneous wetting situations? The interesting idea of making hygrophobic surfaces from hygrophilic materials was suggested[43] and demonstrated[1–3,8] without considering the feasibility condition, eq 21. However, as will be shown below, the role of this condition is crucial in determining whether this idea is possible.

In principle, eq 15a shows that in order to get equilibrium in the heterogeneous regime for a rough, hygrophilic material ($\cos\theta_Y>0$) the derivative, df_l/dz, must be positive. This is so, since df_{sl}/dz is positive by definition. Thus, such an equilibrium state may be achieved at the positions where the liquid−air interfacial area increases upon further penetration. Referring to the simple examples in Figure 1a, these positions would be located at the lower part of the convex features (e.g., as in Figure 1c) or the upper part of the concave features. For roughness topographies that combine both convex and concave features, there may be multiple equilibrium positions.

However, to determine whether these states are in stable or unstable equilibrium, eq 21 is needed. Clearly, this equation indicates that d^2f_l/dz^2 should be as high as possible and d^2f_{sl}/dz^2 should be as low as possible for the equilibrium to be stable when a hygrophilic material is used. However, it appears to be difficult to derive general conclusions from the feasibility condition for all types of surface topographies, mainly because it involves second derivatives. Therefore, while eq 21 is general for all roughness topographies, it is reasonable to first study very simplified, specific examples that will yield hints about the expected behavior in more general situations.

Two very simplified geometries will be studied below: cylindrical (two-dimensional) grooves and cylindrical protrusions (please note that the two-dimensional nature of the roughness features in these two examples does not imply that the drops put on the surface are two-dimensional). For the cylindrical grooves, simple calculations lead to

$$(f_{sl})_{cg} = 1 - 2\rho \sin \varphi_o + 2\rho(\varphi - \varphi_o) \quad (22)$$

where the subscript cg stands for cylindrical groove, ρ (<0.5) is the radius of the circular cross section of the groove, given as a fraction of the size of the unit cell of the surface, φ is the angle between the radius connecting to a given point on the circle and the vertical axis, and φ_o is the value of φ at the groove opening (see Figure 2a for the definitions of the geometric parameters). The derivatives of f_{sl} are given by

$$\frac{d(f_{sl})_{cg}}{dz} = \frac{2}{\sin \varphi} \quad (23)$$

$$\frac{d^2(f_{sl})_{cg}}{dz^2} = -\frac{2\cos \varphi}{\rho \sin^3 \varphi} \quad (24)$$

In addition

$$(f_l)_{cg} = 2\rho \sin \varphi \quad (25)$$

$$\frac{d(f_l)_{cg}}{dz} = 2\cot \varphi \quad (26)$$

$$\frac{d^2(f_l)_{cg}}{dz^2} = -\frac{2}{\rho \sin^3 \varphi} \quad (27)$$

Figure 3 demonstrates the multivalued nature of the dependence of $(f_{sl})_{cg}$ on $(f_l)_{cg}$.

The equilibrium condition, eq 15a, turns into

$$\frac{d(f_{sl})_{cg}/dz}{d(f_l)_{cg}/dz} = \frac{1}{\cos \varphi} = \frac{1}{\cos \theta_Y} \quad (28)$$

and demonstrates that the Young contact angle must be locally achieved ($\varphi = \theta_Y$ at the equilibrium position of the liquid−air interface inside the groove). The feasibility condition, eq 21, together with eqs 24, 27, and 28 leads to

$$\left[\frac{2(\cos^2 \theta_Y - 1)}{\rho \sin^3 \theta_Y}\right]_{cg} > 0 \quad (29)$$

The numerator of the left-hand side of eq 29 is always negative, while the denominator is always positive. Thus, the feasibility condition cannot be fulfilled inside a cylindrical groove, irrespective of its size, opening size, or the Young contact angle. Figure 4a shows an example of the Gibbs energy for a drop on a surface with cylindrical grooves, as it depends on the two independent variables: the extent of penetration into the depth of the roughness, z, and the geometric APCA of the drop, θ. This example ($\rho = 0.2$ and $\theta_Y = 70°$) clearly shows the saddle point and demonstrates the physical meaning of the feasibility condition: even if the local geometric CA inside the groove equals the Young CA, this is not an equilibrium state, since the Gibbs energy is not at a local minimum. Realistic roughness topographies are not necessarily similar to cylindrical grooves, but the present result may suggest that concave parts of roughness topographies may not support equilibrium of the liquid−air interface, even if the local Young CA can be achieved.

For cylindrical protrusions, the required expressions are given in the following (see Figure 2b for the definitions of the geometric parameters). These expressions are valid for $z < Z$, where Z is the height of the protrusion; the case $z = Z$ is not treated here, since it represents the homogeneous (Wenzel) wetting regime.

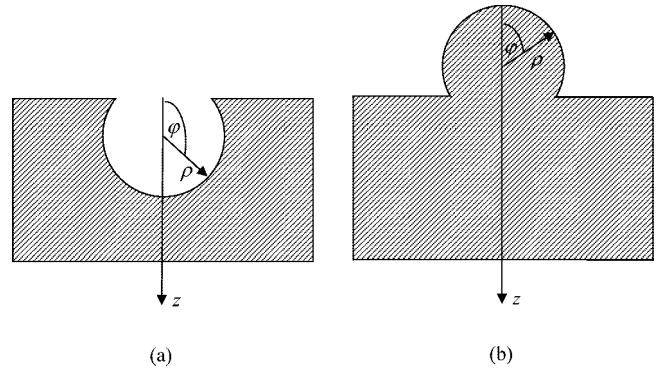

Figure 2. Geometrical definitions of (a) cylindrical grooves and (b) cylindrical protrusions.

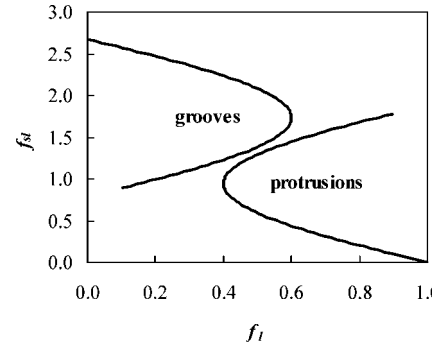

Figure 3. Multiple-valued dependence of f_{sl} on f_l for cylindrical grooves and cylindrical protrusions.

$$(f_{sl})_{cp} = 2\rho\varphi \quad (30)$$

where the subscript cp stands for cylindrical protrusions. The first and second derivatives of f_{sl} in this case are identical to those given by 23 and 24, respectively:

$$\frac{d(f_{sl})_{cp}}{dz} = \frac{2}{\sin \varphi} \quad (31)$$

$$\frac{d^2(f_{sl})_{cp}}{dz^2} = -\frac{2\cos \varphi}{\rho \sin^3 \varphi} \quad (32)$$

In addition

$$(f_l)_{cp} = 1 - 2\rho \sin \varphi \quad (33)$$

$$\frac{d(f_l)_{cp}}{dz} = -2\cot \varphi \quad (34)$$

$$\frac{d^2(f_l)_{cp}}{dz^2} = \frac{2}{\rho \sin^3 \varphi} \quad (35)$$

Again, the multivalued nature of the dependence of $(f_{sl})_{cp}$ on $(f_l)_{cp}$ is demonstrated in Figure 3.

The equilibrium condition, eq 15a, turns in this case into

$$\frac{d(f_{sl})_{cp}}{df_l} = -\frac{1}{\cos \varphi} = \frac{1}{\cos \theta_Y} \quad (36)$$

and, again, demonstrates that the Young contact angle must be locally achieved ($\varphi = \pi - \theta_Y$ at the equilibrium position). The feasibility condition, eq 21, together with eqs 32, 35, and 36 leads to

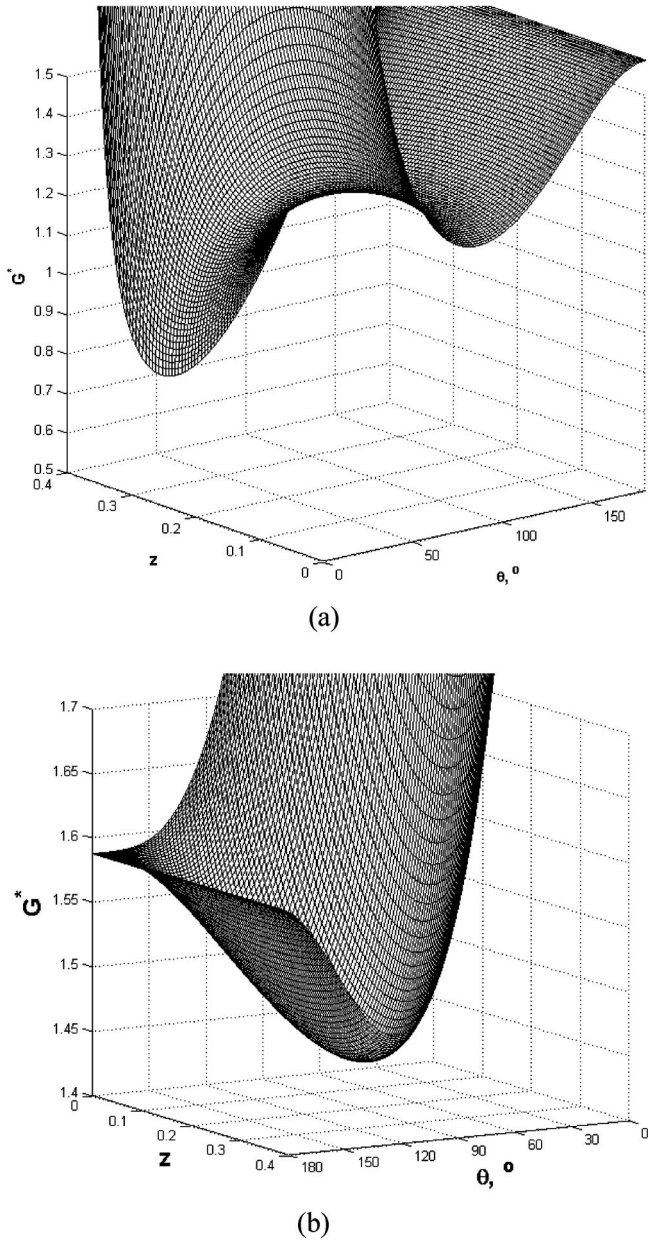

Figure 4. Gibbs energy of the system for (a) a surface with cylindrical grooves and (b) a surface with cylindrical protrusions. $\rho = 0.2$ and $\theta_Y = 70°$. Note the saddle point in (a) and the true local minimum in (b).

$$\left[\frac{2(1-\cos^2\theta_Y)}{\rho\sin^3\theta_Y}\right]_{cp} > 0 \qquad (37)$$

This condition is always fulfilled, so the feasibility condition never denies a CB equilibrium for cylindrical protrusions. For hygrophilic materials, the location of the liquid−air interface at equilibrium must be at the lower parts of the cylindrical protrusions, since only there the local geometric CA may equal the Young CA. Figure 4b shows an example of the Gibbs energy for a drop on a surface with cylindrical protrusions ($\rho = 0.2$ and $\theta_Y = 70°$). This figure clearly shows the local minimum in the Gibbs energy. Again, realistic roughness topographies are usually not similar to cylindrical protrusions, but this result may hint that the lower convex parts of multivalued roughness topographies may support equilibrium of the liquid−air interface for Young CAs that are lower than 90°.

For surfaces with cylindrical protrusions, the CB equation turns into

$$\cos\theta_{CB} = 2\rho[\sin\theta_Y + (\pi - \theta_Y)\cos\theta_Y] - 1 \qquad (38)$$

In order for the surface to appear hygrophobic ($\cos\theta_{CB} < 0$)

$$\rho < \frac{1}{2[\sin\theta_Y + (\pi - \theta_Y)\cos\theta_Y]} \qquad (39)$$

This equation shows that the possibility of making a hygrophobic surface from a hygrophilic material for cylindrical protrusions depends on the radius of the protrusion relative to the unit cell size: the smaller the radius, the more hygrophobic the surface. This makes sense, since the more distant are the protrusions from each other there is more room for a liquid−air interface, which is the source of hygrophobicity. For Young contact angles of 90° and above, any radius of the cylindrical protrusions may lead to a hygrophobic surface ($\cos\theta_{CB} < 0$). This is so, since for $\theta_Y = 90°$ ρ should be less than 0.5, which is true anyway, by definition. For the extreme case of a completely hygrophilic material, $\theta_Y = 0°$, it may, in theory, be possible to get a hygrophobic surface if ρ is smaller than $1/(2\pi) = 0.159$. The practicality of this surprising result is discussed below. For any intermediate case of a hygrophilic material ($0 < \theta_Y < 90°$), the theoretical possibility of making a hygrophobic surface of cylindrical protrusions is given by eq 39, based on the corresponding maximum value of ρ.

Figure 5 demonstrates the specific predictions of eq 38 by showing the CB APCAs for two values of the dimensionless radius of the cylindrical protrusions. These calculations were done for protrusions, the cross section of which is almost a full circle, to allow all possible positions for the liquid−air interface. For $\rho = 0.4$, for example, the effect is mild: hygrophobicity is achieved only for $\theta_Y > \sim 81°$, and CAs needed for superhygrophobicity ($\theta_{CB} > 150°$) cannot be achieved with currently available materials ($\theta_Y < \sim 120°$). However, for $\rho = 0.2$, the results are much better: hygrophobicity is achieved for $\theta_Y > \sim 41°$, and the lower limit of the CA required for superhygrophobicity is reached for $\theta_Y = \sim 120°$. As mentioned above, for this very simplified example of cylindrical protrusions, the hygrophobic state is achieved when the liquid−air interface is located at the lower parts of the protrusions. The more hygrophilic the material (the lower the Young CA), the closer the liquid−air interface must be to the bottom of the protrusion. For example, in the extreme case of $\theta_Y = 0°$, the protrusion has to be a complete circle, and the liquid−air interface must touch it at the bottom. This is, obviously, impractical, since the liquid−air interface cannot stay stable at a zero distance from the base solid surface without wetting it and getting the drop into the Wenzel regime. So, keeping a distance between the liquid−air interface and the base solid surface is practically possible only for Young CAs above a certain value, which needs to be determined for each specific case.

Moreover, the existence of hygrophobic surfaces made from hygrophilic materials is not only a question of thermodynamic feasibility. It is also a question of thermodynamic stability.[19] The energy of the drop in the heterogeneous wetting (CB) regime has to be compared with the energy in the homogeneous (Wenzel) regime; the state that leads to the lower CA turns out to be the more stable one. The Wenzel equation for the simplified example of surfaces with cylindrical protrusions is given by

$$\cos\theta_W = [1 + 2\rho(\varphi_Z - \sin\varphi_Z)]\cos\theta_Y \qquad (40)$$

where φ_Z is the value of φ at the protrusion base ($z = Z$). Figure 5 demonstrates the comparison between the CB and Wenzel

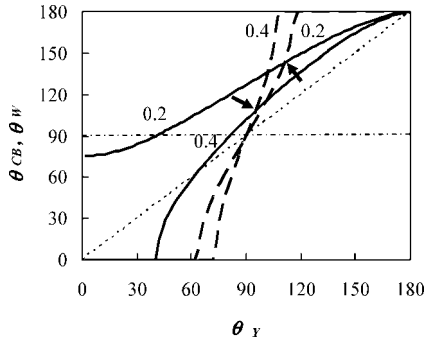

Figure 5. CB (full lines) and Wenzel (dashed lines) contact angles for a surface made of cylindrical protrusions. The numbers indicate the normalized radius of a protrusion. The arrows indicate the transition points between the two regimes. Also shown, by thin dotted lines, are the line of equality between the APCA and the Young CA, and the line at an APCA of 90° that distinguishes between hygrophilicity and hygrophobicity.

APCAs for such surfaces. The point where the Wenzel and the CB lines cross each other is the transition between the two regimes (see arrows in Figure 5). As mentioned above, the value of φ_Z for these calculations was taken as 180° (full circle), since the transition points were found out to be relatively insensitive to this value. It can be seen that, when ρ is smaller (higher θ_{CB}), the transition between the two regimes occurs at a higher value of θ_Y. Thus, the stability consideration may have a negative effect on the possibility of making hygrophobic surfaces from hygrophilic materials. Again, this conclusion is quantitatively derived here for a very simplified roughness topography in order to point out the problem. The implications of this point will have to be studied separately for each specific topography.

As stated in the Introduction, a superhygrophobic (liquid-repellent) surface is defined by a sufficiently high APCA and a sufficiently low roll-off angle. The latter is achieved when CA hysteresis is minimized, since then it is difficult for a drop sitting on a tilted surface to find an equilibrium position for both its front and back ends. The CB regime for "regular," single-valued roughness topographies offers a solution to both requirements. First, the APCA is high due to the large area fraction of the drop base that is exposed to the air inside the roughness valleys (low value of f in eq 2). Second, for the same reason, hysteresis is minimized by the homogeneity of the liquid−air interface inside these valleys. The situation may be more complex with multivalued roughness topographies, since the liquid−air interface must penetrate more deeply into the roughness valleys (e.g., in the cylindrical protrusions case, it must be located at the lower parts of the protrusions). Consequently, the solid−liquid interfacial area seems to necessarily be larger than in the single-valued roughness case, and hysteresis may be more pronounced. The calculation of the hysteresis range is beyond the scope of the present paper; however, it is clear that the challenge of designing a superhygrophobic surface from a hygrophilic material requires optimization of the topography in such a way that hysteresis will be minimized while the APCA will be maximized.

Summary and Conclusions

It is, in theory, possible to make a hygrophobic (or even superhygrophobic) surface from a hygrophilic material if the roughness topography is multivalued. The hygrophobicity in such situations is based on the heterogeneous wetting regime, where air is trapped beneath the liquid inside the roughness valleys. The present theoretical discussion thus supports experimental observations of such situations.[1−3,8]

However, not every multivalued topography can support the heterogeneous wetting regime, even if the local Young CA can be materialized inside the roughness valleys. It does happen only if the feasibility condition, eq 21, is fulfilled, which means that the Gibbs energy does not have a saddle point. This conclusion is the main novel result of the present analysis.

The present calculations were done for two examples of very simplified roughness topographies. The analysis needs to be repeated for each specific topography; however, the present results seem to suggest that concave parts of roughness topographies may not enable a CB state, while convex roughness features may enable the formation of hygrophobic surfaces from hygrophilic materials. The liquid−air interface needs to be located at the lower parts of the convex features in order to make the actual CA inside the roughness valleys equal to the Young CA.

Even when the heterogeneous wetting regime may be feasible on a surface made from a hygrophilic material, the question of stability may hamper the usefulness of the system. A comparison with the energy of the homogeneous wetting regime needs to be made in each case to determine which of the regimes is more stable. The challenge in forming hygrophobic surfaces from hygrophilic materials seems to lie in designing surface topographies that will lead to a very high contact angle that is also stable. An additional part of the challenge is to form a surface that will have minimal CA hysteresis in order to lower as much as possible the roll-off angle.

Acknowledgment. The author thanks the staff of the Greek embassy in Tel Aviv for suggesting the prefix *hygro-* and Mr. Eyal Bittoun for assistance in drawing the three-dimensional energy figures. The author also acknowledges partial support from the AMBIO project (NMP-CT-2005-011827) funded by the European Commission's sixth Framework Programme. Views expressed in this publication reflect only the views of the author, and the Commission is not liable for any use that may be made of information contained therein.

LA800304R